

Fabrication of polymer derived ceramic parts by selective laser curing

T. Friedel^a, N. Travitzky^{a,*}, F. Niebling^b, M. Scheffler^a, P. Greil^a

^a Department of Materials Science, University of Erlangen-Nuernberg, Martensstr. 5, 91058 Erlangen, Germany

^b Department of Manufacturing Technology, University of Erlangen-Nuernberg, 91058 Erlangen, Germany

Available online 15 September 2004

Abstract

Polymer derived ceramic parts of complex shape were fabricated by selective laser curing (SLC). The ceramic parts were built similar to the selective laser sintering process by sequentially irradiating layers consisting of SiC loaded polysiloxane powder with a CO₂-laser beam ($\lambda = 10.6 \mu\text{m}$), which locally induces curing reaction of the polymer phase at moderate temperatures around 400 °C. The laser-cured bodies were converted to Si–O–C/SiC ceramic parts in a subsequent pyrolysis treatment at 1200 °C in argon atmosphere. The scanning speed and the power of the CO₂-laser beam were varied, leading to pronounced differences in material properties. Laser irradiating a powder mixture containing 50 vol.% polymer/50 vol.% SiC resulted in relative green densities between 38 and 60%. Relative densities decreased to 32–50% after pyrolysis due to the polymer shrinkage. A post-infiltration with liquid silicon was carried out in order to produce dense parts. While before infiltration the bending strength only attained 17 MPa as a result of both microcracks in the Si–O–C matrix and a pronounced porosity, an average value of 220 MPa was achieved after post-infiltrating with Si. In the case of 50 vol.% SiC content the linear shrinkage after pyrolysis was only 3%. Thus, the SLC approach can be considered as a near-net-shape forming process of ceramic components with complex geometries. © 2004 Elsevier Ltd. All rights reserved.

Keywords: Rapid prototyping; SLC approach; Polymer derived ceramics

1. Introduction

Since for small-scale manufacturing and prototyping the expenses for models and moulds are crucial factors in the production costs, it is difficult to implement new designs quickly in test parts. Therefore, several techniques have been developed since the late 1980's in order to produce components directly from computer-aided-design (CAD) files without hard tooling, dies or moulds. Most of these so-called rapid prototyping (RP) techniques have been commercialized for the fabrication of plastic and metal parts. However, up to now there have only been few systems available for the production of functional-quality ceramic components. This is hindering for the introduction of new parts because staggering tooling costs frequently prohibit the generation of ceramic prototypes and hence their subsequent application. For this reason, research has been done during

the last years to develop rapid prototyping methods that allow the fabrication of ceramic components. In general, already existing RP techniques have been adapted for the processing of ceramic containing feedstock.^{1–10}

A novel technique called selective laser curing (SLC) has been reported, which is based on the selective laser sintering (SLS) process in which laser radiation is used to build up a ceramic part layer-wise from a powder bed without any shaping device.¹¹ During the SLC process, a thin layer of finely ground powder is spread onto a working platform. The laser energy is directed onto the powder by a scanning system where it locally melts and simultaneously cures a preceramic polymer via its reactive groups. Then the working platform is lowered, a new covering of powder is spread and the scanning repeated. Upon the following pyrolysis of the green part, the preceramic polymer is converted to an amorphous Si–O–C–N ceramic which composition and microstructure depends both on the starting material (e.g. polysiloxanes: Si–O–C, polysilanes: SiC, polysilazanes: Si₃N₄) and additional filler loads (e.g. Cr, MoSi₂, SiC).¹² The incorporation of fillers rigorously reduces the shrinkage

* Corresponding author. Tel.: +49 9131 852 8775; fax: +49 9131 852 8311.

E-mail address: travitzky@ww.uni-erlangen.de (N. Travitzky).

associated with the polymer to ceramic conversion. The near-net-shape manufacturing of bulk ceramic components from organosilicon preceramic polymers mixed with fillers has already been demonstrated. The technologies applied originate from the processing of polymers and include, e.g. injection moulding and hot pressing.^{12–15}

There are two fundamental advantages of the SLC method over other RP, respectively, SLS techniques determined to fabricate ceramics: First of all, most of the RP processes use a polymeric binder phase to stabilise the shape of a ceramic powder part, and hence the shrinkage upon pyrolysis for these systems is large, thus prohibiting near-net-shape manufacturing. However, there is no need to remove the binder in the SLC route, and therefore, the shrinkage associated with the subsequent furnace treatment is very low. Secondly, SLS techniques offering near-net-shape manufacturing properties by omitting the binder phase require high temperatures in the laser spot to trigger sintering since the ceramic particles need to be partially melted. The resulting large temperature gradients can cause considerable residual stresses in the part leading to delamination and distortion. In the SLC process, however, significantly lower temperatures are applied (less than 400 °C) and thermal gradient induced damaging is reduced and dimensional accuracy improved.

The aim of the present work was to investigate SLC processing of filler loaded polysiloxanes for manufacturing of multilayer components. Furthermore, the feasibility of infiltrating the porous components with liquid silicon to obtain dense composite materials was analysed.

2. Experimental procedure

A polymethylsilsesquioxan (PMS) $[(\text{CH}_3)_{0.96}(\text{OH})_{0.036}(\text{OC}_2\text{H}_5)_{0.004}\text{SiO}_{1.5}]_n$ with $n \approx 140$ (Wacker Siliconharz MK, Wacker-Chemie GmbH, Burghausen, Germany) was used as a ceramic precursor. At room temperature the PMS is a powder with a mean particle size of 8.5 μm and a melting point of approximately 60 °C. The functional hydroxyl- and ethoxyl-groups give rise to a condensation curing reaction when the polymer is heated to 150–250 °C and the thermoplastic resin is transformed into a thermosetting material. To accelerate the curing reaction 1 wt.%—based upon the PMS—of aluminium-acetylacetonat $\text{C}_{15}\text{H}_{21}\text{AlO}_6$ (Merck, Darmstadt, Germany) was added as a catalyst. By heating the PMS in inert atmosphere, a complex series of polymer decomposition and structural rearrangement reactions takes place.^{16–19} Between 300 and 800 °C this is accompanied by releasing CH_4 and H_2 , further heating-up leads to the formation of an amorphous oxycarbide network with excess carbon embedded in an amorphous Si–O–C ceramic matrix. The ceramic residue after pyrolysis at 1100 °C consists of roughly 32 mol% Si, 48 mol% O and 20 mol% C.²⁰

SiC (SiC 500 B, H. C. Starck, Selb, Germany) having an average diameter of 17 μm was used as filler. It neither reacts with the polymer nor the glass matrix and hence is an inert

filler. The batch was composed of 40, 50 or 60 vol.% SiC and was thoroughly dry-mixed by ball-milling and applied on the working platform as 100 μm high layers. Melting and curing the powder was done by laser-irradiating with line energies $E_L = 5.6 \dots 22.4 \text{ Ws/m}$ whereas the laser power was either 2.8 or 5.6 W and the scanning speed either 250 or 500 mm/s ($E_L = \text{power of laser/scanning speed}$). The CO_2 -laser used has a wavelength of 10.6 μm (EOSINT M 250, EOS GmbH, Planegg, Germany).

The subsequent pyrolysis in flowing Ar was carried out in three steps, the heating rates were 10 °C/min: 1 h at 220 °C for complete curing, 1 h at 500 °C for release of gases and 3 h at 1200 °C in order to develop a stable oxycarbide ceramic residue. Spontaneous infiltration with liquid silicon (Sigrain HQ, Elkem, Majorstuen, Norway), driven by capillary forces, was accomplished under vacuum at 1500 °C within few minutes. The samples were characterized by density, X-ray analysis (Kristalloflex, Siemens AG, Germany), SE-microscopy (FEI Quanta 200, Germany) and EDX (Oxford Instruments, Inca x-sight, UK). A TGA-analysis of the non-irradiated PMS was conducted under the heat treatment stated above (Netzsch STA 409, Selb, Germany). The strength was evaluated in four-point bending (inner span: 20 mm, outer span: 40 mm) normal to the layer direction with the use of a universal testing machine (Instron 4204, Instron Corp., Canton, USA). The crosshead speed was 0.5 mm/min. For every measurement 10 bars with the dimensions 50 mm \times 4 mm \times 3 mm were prepared by grinding and polishing.

3. Results and discussion

The amount of laser energy applied during the selective laser irradiation is a crucial factor for the microstructure formation and hence the material properties. While line energies below 10 Ws/m result in insufficient melting and curing of the polymer, excess line energies, on the other side, cause the PMS to burn when the process is operated under ambient air. Moreover, the excess energy leads to the melting of adjacent areas in the powder bed, thereby limiting the accuracy of the laser-cured part. Fig. 1 shows the ceramic yield of the PMS in the ceramic matrix composite obtained after subsequent pyrolysis. Four different laser parameters were applied indicating a decrease in ceramic yield with rising E_L . It is also worth noting that varying laser power and scanning speed at a constant line energy leads to different outcomes. Irradiating with 11.2 Ws/m at a power of 5.6 W results in a considerably lower ceramic yield compared to the sample treated at 2.8 W. The maximum ceramic residue of approximately 82 wt.% (measured by TGA-analysis) is achieved by $E_L = 5.6 \text{ Ws/m}$, but the degree of cross-linking in this sample is insufficient to stabilise the part during the pyrolysis because the PMS starts melting at the post heat treatment. Preliminary tests according to a thermo-barometric analysis technique found a degree of curing of at least 35% to be

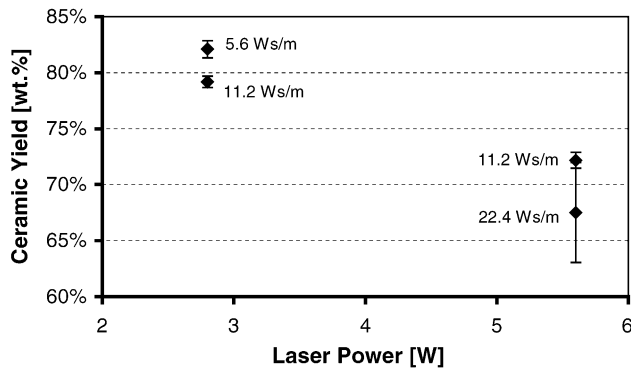


Fig. 1. Ceramic yield of PMS after pyrolysis, starting batch: 50 vol.% PMS/50 vol.% SiC.

necessary to maintain the geometrical shape of a laser-cured part.¹¹

Fig. 2 presents the relative densities of both laser-cured and pyrolysed samples. A maximum green density of 60% is achieved at 11.2 Ws/m (2.8 W, 250 mm/s); both lower and higher line energies lead to significantly reduced relative densities: either insufficient compaction of the powder occurs at 5.6 Ws/m or decomposition of the PMS at 22.4 Ws/m takes place. It is noteworthy that varying laser parameters at a constant line energy of $E_L = 11.2$ Ws/m results in different densities because the heat development over time differs in the powder bed. An increased laser power combined with a faster scanning speed (5.6 W and 500 mm/s instead of 2.8 W and 250 mm/s) will lead to a higher peak temperature and a more rapid cooling. Consequently, the PMS decomposes more easily and the time for powder compaction is shorter, both causing a reduced density.

Although shrinkage of the samples occurs during the subsequent pyrolysis, the porosity increases due to the pronounced volume shrinkage of the PMS, which is roughly 50%. According to Fig. 2, a maximum relative density of 50% can be achieved after the heat treatment.

The relative densities decrease with increasing filler content as it is shown in Fig. 3. Since the compaction of the

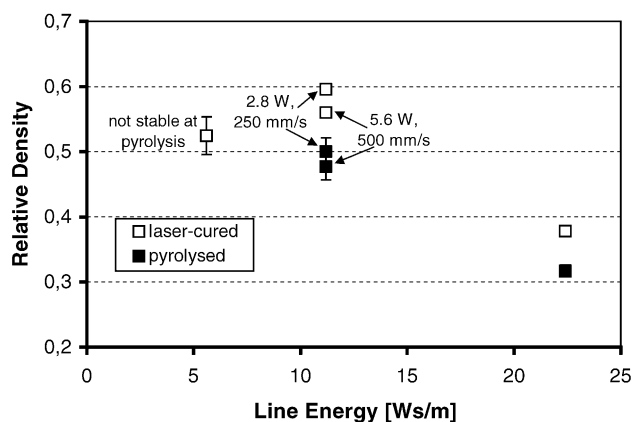


Fig. 2. Relative density of samples, starting batch: 50 vol.% PMS/50 vol.% SiC.

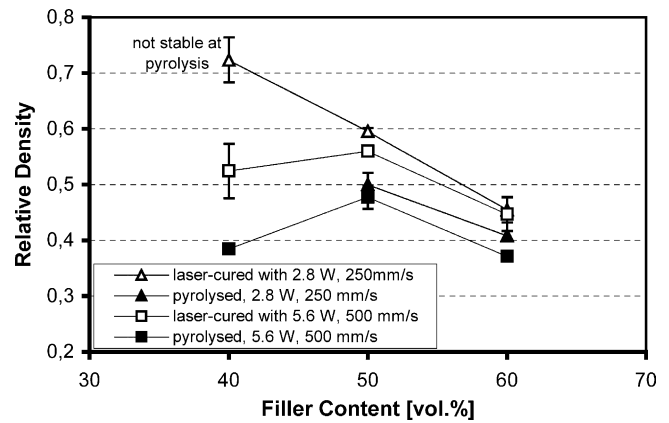


Fig. 3. Relative density of samples, $E_L = 11.2$ Ws/m.

powder during laser irradiation is accomplished by the molten PMS, a higher polymer content gives rise to less porosity in the green part. Even after pyrolysis, the relative density of a sample with 50 vol.% SiC is higher than of a sample containing 60 vol.% SiC despite the greater increase in porosity due to the polymer shrinkage in the former case. Fig. 3 also shows the rising susceptibility to polymer decomposition in batches containing a low filler fraction. The difference between the density of samples irradiated with 2.8 W/250 mm/s compared to 5.6 W/500 mm/s increases with decreasing SiC content. On the basis of similar heat capacities ($c_p \approx 800$ – 1200 J/kg K) but a much higher heat conductivity of the filler ($\lambda \approx 150$ Wm/K) in comparison to the polymer ($\lambda \approx 0.2$ Wm/K), excess heat is more easily compensated if the filler fraction is large and hence burning of the PMS is significantly reduced.

Fig. 4 shows fractured surfaces of samples prepared from the starting batch 50 vol.% PMS/50 vol.% SiC, the powder was laser-cured with $E_L = 11.2$ Ws/m. The fillers are well embedded in the polymer matrix since molten PMS wets SiC easily (wetting angles between 20° and 30° were measured). After pyrolysis, the apparent shrinkage of the polymer leads to an amorphous Si–O–C matrix with small microcracks. XRD-analysis showed no signs of crystallinity in the oxycarbide phase for crystallisation of Si–O–C glasses occurs at elevated temperatures ($>1400^\circ\text{C}$).^{18,19}

Despite the shrinkage of the PMS, the microstructure of green samples maintains throughout pyrolysis as T_g of Si–O–C glass is around 1350°C ,¹⁸ and therefore, no viscous sintering occurs. The effect of varying laser parameters on the microstructure of pyrolysed samples is demonstrated in Fig. 5. A higher scanning speed at constant line energy leads to smaller pores and a more homogeneous structure whereas a lower scanning speed results in large dense regions and pronounced pores. The length of time, in which the PMS remains molten, is crucial for the development of the structure. A longer period of time allows a more advanced rearrangement of the SiC particles and the molten PMS, since the mixture tends to pull together to dense regions. It is noteworthy

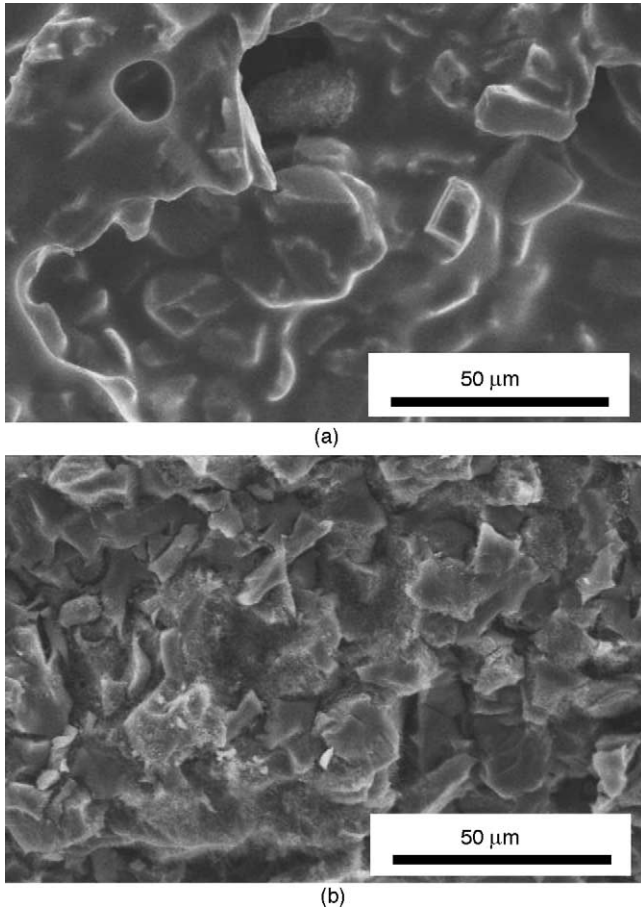
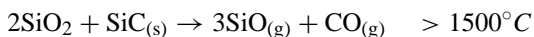
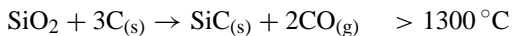


Fig. 4. REM micrographs of fractured surfaces of samples laser-cured with $E_L = 11.2$ Ws/m, (a) before pyrolysis and (b) after pyrolysis; starting batch: 50 vol.% PMS/50 vol.% SiC.

that both samples shown in Fig. 5 have similar densities as is displayed in Fig. 2.

After pyrolysis, the samples were infiltrated spontaneously with liquid silicon at 1500°C due to capillary forces of the open pore channel system. Fig. 6 shows a typical microstructure of an infiltrated specimen, almost no porosity is observable in the sample. The Si–O–C-phase, however, virtually disappeared during the infiltration and could not be detected by SEM and EDX analysis anymore. As a result of the carbothermal reduction which occurs above 1300°C , the Si–O–C matrix was chemically not stable and decomposed to gaseous SiO and CO^{21} due to the following reactions:



Therefore, the volume fraction of the infiltrated silicon not only corresponds to the former pore volume ($\approx 50\%$) but increases to approximately 65% since the oxycarbide matrix accounted for 15.5% of the total sample volume prior to infiltration.

In order to demonstrate the capability of the SLC-process, a downscaled turbine wheel was manufactured from the start-

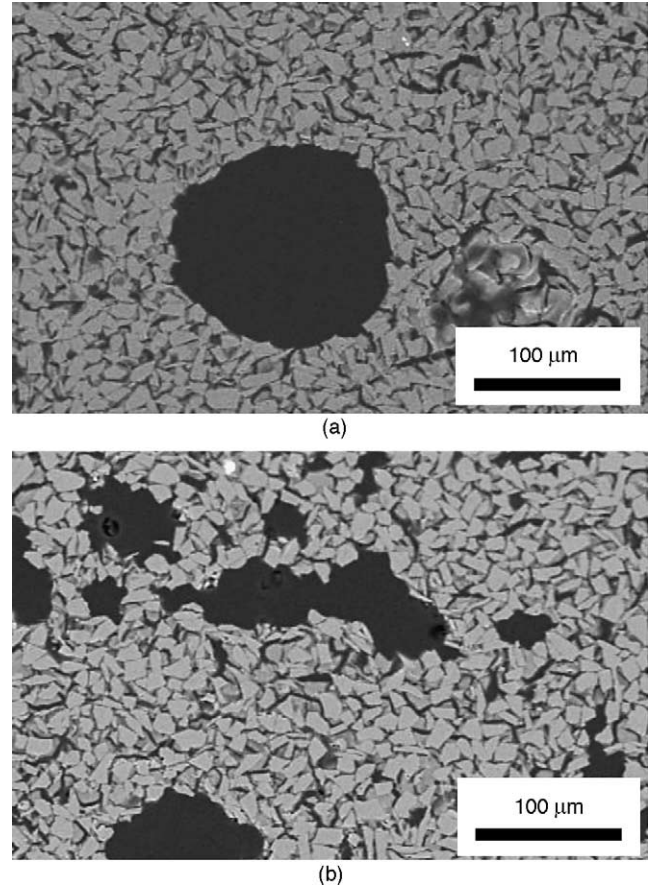


Fig. 5. REM micrographs of samples laser-cured with $E_L = 11.2$ Ws/m and pyrolysed, (a) 2.8 W and 250 mm/s, (b) 5.6 W and 500 mm/s; starting batch: 50 vol.% PMS/50 vol.% SiC. The dark grey phase is resin, which was infiltrated in the open porosity prior to grinding and polishing.

ing batch 50 vol.% PMS/50 vol.% SiC. The automatic generation of the component via a 3D-CAD file is shown in Fig. 7. All details of the part can be maintained and a bending strength of 2.0 ± 0.1 MPa is sufficient to handle it safely

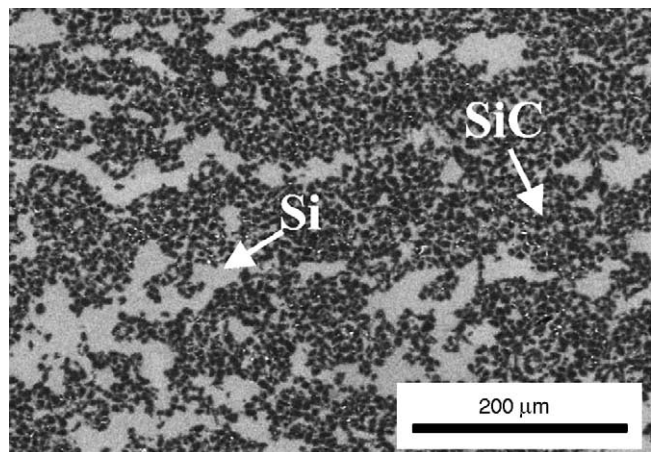


Fig. 6. REM micrograph of a sample laser-cured with $E_L = 11.2$ Ws/m, pyrolysed and infiltrated with silicon; starting batch: 50 vol.% PMS/50 vol.% SiC.

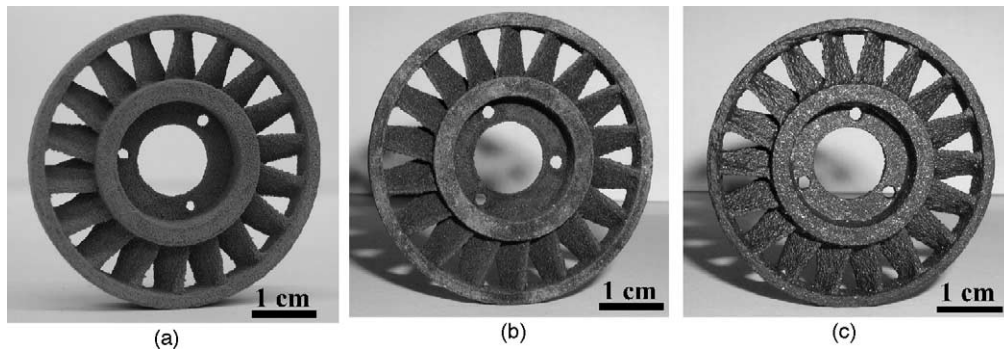


Fig. 7. Downscaled turbine wheel: (a) laser-cured with $E_L = 11.2 \text{ Ws/m}$, (b) pyrolysed, and (c) infiltrated with silicon; starting batch: 50 vol.% PMS/50 vol.% SiC.

during post-processing. The pyrolysis is accompanied by a shrinkage of only 3.3% in diameter, no distortion of the part occurs. The strength of $17 \pm 1.4 \text{ MPa}$ is quite low due to a porosity of 50 vol.% and microcracks in the Si–O–C matrix. After infiltrating with silicon, the geometrical shape of the part is preserved and no further shrinkage takes place. The bending strength raises to $220 \pm 14 \text{ MPa}$ which is typical for SiSiC ceramics consisting of 65 vol.% Si.²² The density of the part is 2.64 g/cm^3 and no porosity can be observed.

4. Conclusions

The influence of the laser scanning parameters and the filler content on the microstructure and strength of manufactured samples were demonstrated. The successful conversion of a CAD-file to a green part by selective laser curing followed by pyrolysis and infiltration could be shown. A low linear shrinkage of 3.3% occurred mainly upon pyrolysis whereas an almost invariant dimensional change accompanied the final Si-infiltration. The fracture strength of laser-cured samples of 2.0 MPa increased after pyrolysis to 17 MPa and attained 220 MPa by infiltrating the porous component with liquid silicon.

Acknowledgement

The authors gratefully acknowledge the Deutsche Forschungsgemeinschaft DFG for financial support.

References

- Chartier, T., Chaput, C. and Doreau, F., *J. Mater. Sci.*, 2002, **37**(15), 3141.
- Zimbeck, W., Pope, M. and Rice, R., In *Proceedings of the Solid Freeform Fabrication Symposium Austin*. University of Texas at Austin, 1996, p. 411.
- Seerden, K., Reis, N. and Evans, J. G., *J. Am. Ceram. Soc.*, 2001, **84**(11), 2514.
- Mott, M. and Evans, J., *J. Am. Ceram. Soc.*, 2001, **84**(2), 307.
- Vaidyanathan, R., Walsh, J. and Lombardi (Member), J., *J. Miner. Metals Mater. Soc.*, 2000, **12**, 34.
- Agarwala, M., van Weeren, R. and Bandyopadhyay, A., In *Proceedings of the Solid Freeform Fabrication Symposium Austin*. University of Texas at Austin, 1996, p. 335 (in press).
- Klosterman, D., Chartoff, R. and Priore, B., In *Proceedings of the Solid Freeform Fabrication Symposium Austin*. University of Texas at Austin, 1996, p. 105.
- Rodrigues, S., Chartoff, R. and Klosterman, D., In *Proceedings of the Solid Freeform Fabrication Symposium Austin*. University of Texas at Austin, 2000, p. 1.
- Löschau, H., Lenk, R. and Scharek, S., In *Proceedings of the 9th CIMTEC—World Ceramic Congress and Forum on New Materials, Florence, Italy, June 14–19, Part B*, 1998, p. 567.
- Stierlen, P., *Rapid Prototyping von Keramiken—Entwicklung eines Verfahrens zur Herstellung reaktionsgebundener SiSiC-Prototypen*. Dissertation, Universität Stuttgart, Shaker Verlag, Aachen, 2002.
- Sindelar, R., Buhler, P., Niebling, F., Otto, A. and Greil, P., In *Proceedings of the Solid Freeform Fabrication Symposium Austin*. University of Texas at Austin, 2002, p. 133.
- Greil, P., *J. Am. Ceram. Soc.*, 1995, **78**(4), 835.
- Kaindl, A., Lehner, W., Greil, P. and Kim, D.-J., *Mater. Sci. Eng. A*, 1999, **260**, 101.
- Cromme, P., Scheffler, M. and Greil, P., *Adv. Eng. Mater.*, 2002, **4**, 873.
- Dernovsek, O., Bressiani, J. C., Acchar, W. and Greil, P., *J. Mater. Sci.*, 2000, **35**, 2201.
- Belot, V., Corriu, R. J., Leclercq, D. and Mutin, P. H., *J. Polym. Sci. Part A: Polym. Chem.*, 1992, **30**, 613.
- Gualandris, V., Hourlier-Bahloul, D. and Babonneau, F., *J. Sol-Gel Sci. Technol.*, 1999, **14**, 39.
- Renlund, G. M. and Prochazka, S., *J. Mater. Res.*, 1991, **6**(12), 2723.
- Pantano, C. G., Singh, A. K. and Zhang, H., *J. Sol-Gel Sci. Technol.*, 1999, **14**, 7.
- Scheffler, M., Gambaryan-Roisman, T. and Takahashi, T., *Ceram. Trans.*, 2000, **115**, 239.
- Sorarù, G. D. and Suttor, D., *J. Sol-Gel Sci. Technol.*, 1999, **14**, 69.
- Lee, W. E. and Rainforth, W. M., *Ceramic Microstructures*. Chapman & Hall, London, 1994, p. 427.